COAXIAL COUPLER RF KICK IN THE PITZ RF GUN

Y. Chen†, H. Qian, M. Krasilnikov, I. Isaev, Q. Zhao[1], P. Boonpornprasert, J. Good, H. Huck, A. Oppelt, Y. Renier and F. Stephan, DESY, Platanenallee 6, 15738 Zeuthen, Germany
W. Ackermann, H. De Gersem, TEMF, Technische Universität Darmstadt, Schlossgartenstraße 8, 64289 Darmstadt, Germany
M. Dohlus, DESY, Notkestraße 85, 22607 Hamburg, Germany

Abstract

We investigate a transverse RF kick induced by the transition between rectangular waveguide and coaxial line of the RF coupler in the 1.6-cell L-band normal conducting (NC) RF gun at the Photo Injector Test Facility at DESY, Zeuthen site (PITZ). A three-dimensional electromagnetic simulation shows the disturbed RF field distributions in the fundamental accelerating mode. Based on the 3D RF field map, an electron beam based characterization and quantification of the coaxial coupler RF kick in the PITZ gun is simulated. The current status of the investigation is presented.

INTRODUCTION

As a high brightness photoelectron source required for the operation of TESLA technology based FELs, the 1.6-cell 1.3-GHz NC RF gun at PITZ has been used at FLASH [1] and the European X-ray Free Electron Laser (XFEL) [2]. The RF power in the PITZ gun is supplied by a 10 MW multi-beam klystron. The power is coupled from the input waveguide (WG) via the door-knob transition into the rotationally symmetric coupler and the gun cavity. This is illustrated in Fig. 1. For a thorough description of the PITZ gun and its supporting RF system, the interested reader is referred to [3-6].

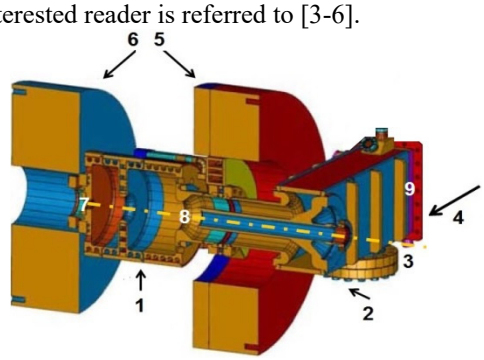

Figure 1: Sketch of the PITZ gun with coaxial RF coupler: 1-gun cavity, 2-door-knob transition, 3-cavity axis, 4-RF feeding direction, 5-main solenoid, 6-bucking solenoid, 7-cathode, 8-end of coaxial line and 9-reference position of WG port for simulations. Note that this sketch is rotated by 90 degrees compared to the computational model used in the follow-up simulations.

† ye.lining.chen@desy.de
[1] on leave from IMP/CAS, Lanzhou, China

The rotationally symmetric coupler at PITZ is designed as a coaxial input coupler that couples to the gun cavity on the cavity axis [7-8]. The axial symmetry of the cavity thus stays undisturbed. Compared to the conventional input coupler aside the cavity [9], the asymmetric electromagnetic modes are strongly suppressed. This inhibits the emittance growth due to the RF field distortions caused by these asymmetric modes. The evanescent dipole modes, however, are not avoidable to be generated at the door-knob transition (see 2 in Fig. 1). The dipole modes may not be fully decayed till the end of the coaxial line and thus can disturb the cylindrical symmetry of the fundamental mode. The induced RF field asymmetries may create a transverse kick onto the electron bunch [10-11]. This occurs, more specifically, when the bunch is leaving the cavity through the inner conductor of the coaxial line (see 8 in Fig. 1). To first clarify the RF field asymmetries, three-dimensional electromagnetic field simulations are performed using CST Microwave Studio® (CST-MWS®) [12].

RF FIELD ASYMMETRY

The RF field in the gun is simulated using the frequency domain solver in CST-MWS®. To enable excitation, a standard WG port condition is applied at the boundary of the input WG. Based on a so-called mono-frequency excitation method, two principal matching conditions (i.e., broadband matching from WG to coaxial line and narrowband matching from coaxial line to cavity) are satisfied by slightly tuning the length of the inner conductor. This results in a reflection coefficient lower than -30 dB at the WG port position. The RF field is then calculated under such optimized conditions of the gun at its resonance frequency. Surface losses are taken into account. Based on the field simulation, a 3D RF field map is also extracted for later particle tracking simulations in ASTRA [13].

In Fig. 2, the RF field asymmetries are exemplarily visualized in the close vicinity of the coaxial coupler. One can recognize these asymmetries from the electric and magnetic field strength variation around the inner conductor, as well as from the on-axis zero-crossing positions of the fields.

ISBN 978-3-95450-179-3

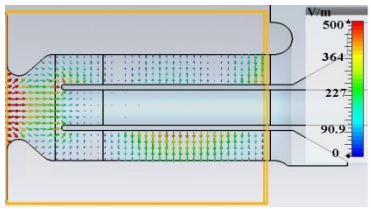

(a) Cut-plane view of E-vector

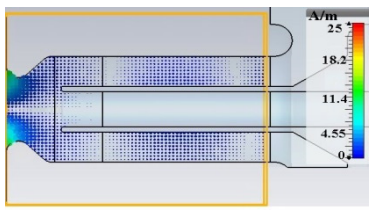

(b) Cut-plane view of H-vector

Figure 2: Illustration of the local RF field asymmetries. The colour maps are adjusted for a better visualization.

Figure 3 shows the distribution of the transverse magnetic field component (Hx) along the cavity axis. Note that the magnetic field starts to rise at about the end of the gun cavity. It reaches the peak value somewhere in the transition between the end of the coaxial line and the cavity. The field distribution is decaying into the inner conductor of the coaxial line. Furthermore, the field is compared to the same field component calculated by a simulation without the door-knob transition and the rectangular waveguide in the computational model. One can see that the resulting Hx component in this case is almost zero. For this comparison, the maximum accelerating electric field in both cases are normalized to 60 MV/m.

In our simulation frame, such an existing horizontal magnetic component (red curve) can kick the electron bunch vertically. In order to know the correlation of the vertical kick with time, particle tracking simulations are performed at different RF phases of the gun using an extracted 3D RF field map.

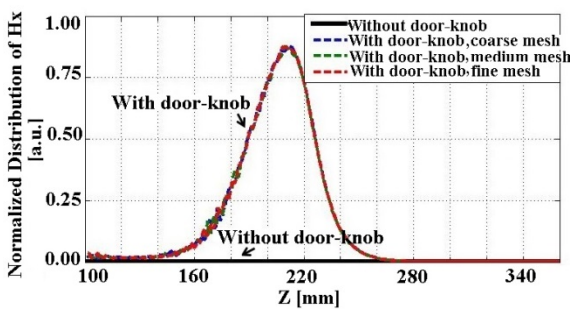

Figure 3: Distribution of the magnetic field component along the cavity axis and the comparison with the same field calculated by a simulation without the door-knob transition and the rectangular waveguide in the computational model. Different curves in colours represent gradual steps for mesh refinements in the simulations.

BEAM-BASED CHARACTERIZATION OF THE RF KICK

The kick characterization is conducted by scanning the RF start-phase of the gun in particle tracking simulations. The beam centroid is initially placed at the center of the cathode plane. It is tracked through the gun cavity till close vicinity of the door-knob transition. The whole calculation domain is covered by the RF field map.

In Fig. 4, the particle offset from the axis on the transverse plane and corresponding transverse momentum are calculated at different longitudinal positions along the cavity axis. A vertical kick is identified starting from the transition of the full cell of the gun to the coaxial line (see (d) in Fig. 4). The kick strength is, furthermore, depending on the start-phase of the gun. At the Maximum Mean Momentum Gain (MMMG) phase (i.e., 40 degrees), this leads to a transverse kick of about 0.65 mrad. A vertical offset of 55 µm is found at 0.3 meters downstream from the photocathode. However, there is almost no considerable kick in the horizontal direction for a large range of the RF phase w.r.t. the MMMG phase of the gun.

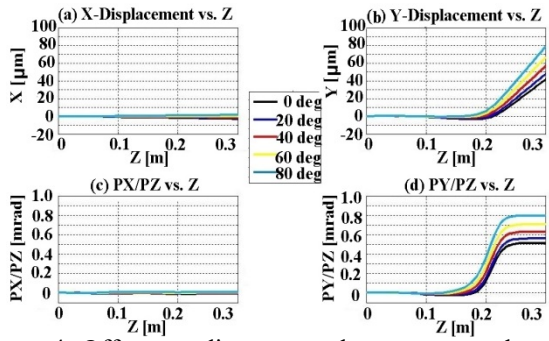

Figure 4: Off-center distance on the transverse plane and corresponding transverse momentum of the beam centroid for the RF start-phases.

In Fig. 5, the kick strength and the particle offset from the axis at z = 0.3 m are plotted as a function of the gun phase. The red star denotes the MMMG phase of the gun. Note that, a nominal electron bunch of 20 ps FWHM (full width half maximum) at PITZ corresponds to about 10 degrees gun phase at the resonant frequency of 1.3 GHz. Consequently, the head and tail of the electron bunch may see a kick slope (see (b) in Fig. 5) due to the time dependency of the RF kick. This results in a kick difference of about 0.05 mrad around the MMMG phase at a RF power level of 6.5 MW in the gun. However, the presence of the imperfect solenoid fields may further complicate the beam dynamics in a nonlinear manner.

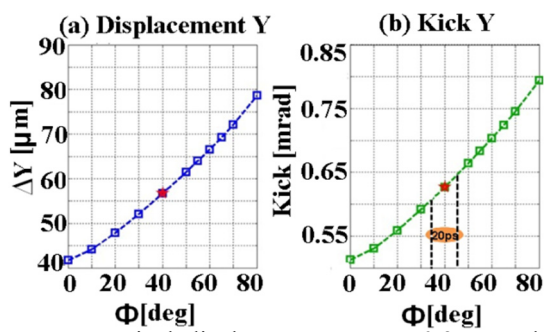

Figure 5: Vertical displacement at z = 0.3 m and kick strength as a function of the gun phase.

ISBN 978-3-95450-179-3

MULTIPOLE-EXPANSION BASED QUANTIFICATION OF THE KICK

To clarify the multipole composition and quantify their strengths in the integral kick, the transverse momentum of the beam particle is presumably decomposed in a dipole component, a normal and a skew quadrupole component according to

$$P_X = P_{0x} + (K_{RF} + K_N)X + K_S Y \quad (1)$$

and

$$P_Y = P_{0y} + (K_{RF} - K_N)Y + K_S X. \quad (2)$$

Here, X and Y are the particle offsets from the axis at the location of the integral kick, respectively. The terms P_X and P_Y represent the particle transverse momenta in the horizontal and vertical direction, respectively. The parameters P_{0x} and P_{0y} characterize the dipole kick while K_{RF} describes the RF focusing strength of the cylindrical symmetric mode. The values K_N and K_s denote the normal and skew quadrupole kick strength, respectively.

The kick strengths of the multipole components in (1-2) are quantified based on the tracking simulations for a grid of macroparticles initially placed on the cathode plane (see Fig. 6). These particles are tracked through the gun cavity passing by the end of the coaxial coupler till the door-knob transition. The whole calculation domain is covered by a 3D RF field map. The simulation results are shown in Fig. 7. The integral transverse RF kick at z = 0.3 m is plotted as a function of the vertical and horizontal displacements at z = 0.18 m for all the simulation particles. A vertical kick is seen in Fig. 7 (b). The transverse momentum in Fig. 7 (a) and (d) is nearly linear proportional to the displacement at the kick location.

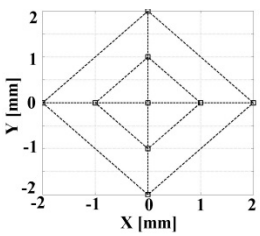

Figure 6: Beam centroid positions on the cathode plane used in the simulations for kick quantification.

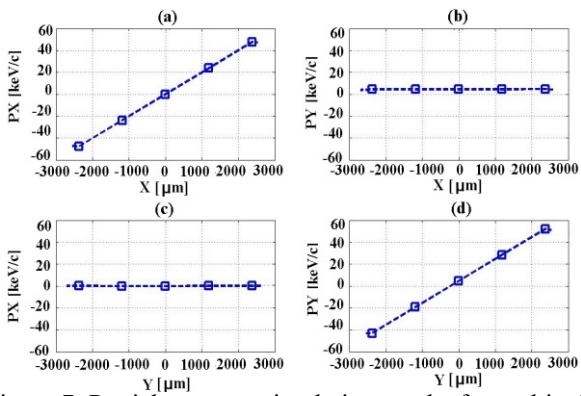

Figure 7: Particle tracking simulation results for multipole-expansion based quantification of the integral kick.

Based on the simulation results in Fig. 7, the multipole-expansion forms (1-2) are numerically fitted. This renders a pronounced vertical dipole kick (P_{0y}) of 4.576 keV/c. The horizontal dipole kick strength (P_{0x}) is almost zero. For the normal quadrupole component, the kick strength K_N is estimated as 1.0e-5 keV/c/μm. The skew quadrupole component is calibrated by K_S as 5.0e-6 keV/c/μm.

Furthermore, to cross-check the kick quantification, an electron bunch of 20 ps is used for tracking simulations, instead of beam centroids. Fig. 8 shows the vertical kick strength as a function of the longitudinal position for the electron bunch distribution at z ≈ 0.33 m (blue dots). To visualize the kick variation in time, the whole bunch is treated slice by slice (dashed black lines). Within each slice, the mean kick strength is calculated. The inset provides a closer look at the trend of the kick slope along the bunch. One can see that the mean kick strength is 0.65 mrad, and also that the bunch tail sees higher kick strength than the head by about 0.05 mrad. This is consistent with the results shown in Figs. 4 and 5.

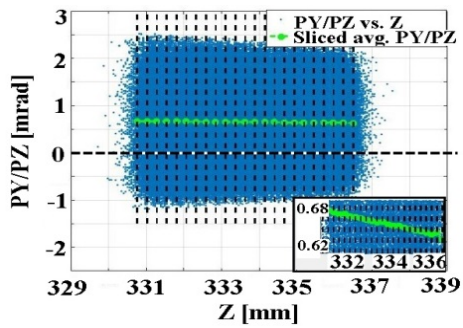

Figure 8: Bunch distribution at z ≈ 0.33 m in terms of the vertical kick strength versus z-positions.

SUMMARY AND OUTLOOK

In this paper, RF fields with rotational symmetry disturbed by the transition from the input rectangular waveguide to the coaxial coupler of the PITZ gun are shown. The resulting RF kick to the electron bunch is vertical and time-dependent. The latter characteristic can introduce a kick slope along the bunch. The integral kick is, furthermore, quantified in the form of its multipole components using the results of particle tracking simulations. This gives a main vertical dipole kick of about 0.65 mrad at the MMMG phase of the gun for a gun RF power of 6.5 MW. A small normal and skew quadrupole component is found to be 1.0e-5 and 5.0e-6 keV/c/μm, respectively. Further studies are foreseen to investigate the impacts of the kick on beam dynamics when space charge effect is included. Note that, to explain the asymmetries in measured transverse phase spaces of the electron bunch at PITZ, other effects, such as the imperfect solenoid symmetry are also under investigation [14-16].

ACKNOWLEDGEMENT

The authors would like to thank Klaus Flöttmann and Frank Brinker from DESY for very useful advices and comments on this topic.

ISBN 978-3-95450-179-3

REFERENCES

[1] W. Ackermann *et al*., "Operation of a free-electron laser from the extreme ultraviolet to the water window", *Nat. Photon*. 1, 336 (2007).

[2] M. Altarelli *et al*., Report No. DESY 2006-097, DESY (2006).

[3] F. Stephan *et al*., "Detailed characterization of electron sources yielding first demonstration of European X-ray Free-Electron Laser beam quality", *PRST-AB* 13, 020704 (2010).

[4] M. Krasilnikov, F. Stephan *et al*., "Experimentally minimized beam emittance from an L-band photoinjector", *PRST-AB* 15, 100701 (2012).

[5] Y. Renier *et al*., "Statistics on high average power operation and results from the electron beam characterization at PITZ", *Proc. IPAC'17*, Copenhagen, Denmark, TUPIK051 (2017).

[6] F. Stephan and M. Krasilnikov, "High Brightness Photo Injectors for Brilliant Light Sources", in *Synchrotron Light Sources and Free-Electron Lasers*, Springer International Publishing Switzerland, ISBN 9783319143941 (2016).

[7] B. Dwersteg *et al*., "RF gun design for the TESLA VUV Free Electron Laser", *NIM* A393, p. 93-95 (1997).

[8] A. Oppelt *et al*., "Tuning, conditioning, and dark current measurements of a new gun cavity at PITZ", *Proc. FEL'06*, Berlin, Germany, THPPH023, p. 609 (2006).

[9] M. Krasilnikov *et al*., "Impact of the RF-Gun Power Coupler on Beam Dynamics," EPAC'02, Paris, France, p. 1640 (2002).

[10] M. Dohlus *et al*., "Coupler kick for very short bunches and its compensation", *Proc. EPAC'08*, Genoa, Italy, p. 580 (2008).

[11] H. Qian *et al*., "Design of a 1.3 GHz Buncher for APEX", *Proc. IPAC'14*, Dresden, Germany, THPRI066, p. 3924 (2014).

[12] CST Computer Simulation Technology AG, https://www.cst.com/.

[13] K. Flöttmann, ASTRA particle tracking code, http://www.desy.de/~mpyflo/.

[14] M. Krasilnikov *et al.*, "Investigations on Electron Beam Imperfections at PITZ", Proc. *LINAC'16*, East Lansing, MI, MOPLR013 (2016).

[15] M. Krasilnikov *et al.*, "Electron beam asymmetry compensation with gun quadrupoles at PITZ", presented at FEL'17, WEP007.

[16] Q. Zhao *et al.*, "Beam asymmetry studies with quadrupole field errors in the PITZ gun section", presented at FEL'17, WEP010.

ISBN 978-3-95450-179-3